



Biodegradable batteries with immobilized electrolyte for transient MEMS

Didi She¹ · Melissa Tsang² · Mark Allen¹

Published online: 12 February 2019
© Springer Science+Business Media, LLC, part of Springer Nature 2019

Abstract

Biodegradable batteries play an important role in fully degradable biomedical or environmental systems. The development of biodegradable batteries faces many challenges including power content, device compactness, performance stability, shelf and functional lifetime. In particular, a key driver in the lifetime and overall size of microfabricated biodegradable batteries is the liquid electrolyte volume. Harnessing liquid from the environment to serve as the battery electrolyte may, therefore, be desirable; however, for stable operation, maintaining a constant electrochemical environment inside the cell is required even in the presence of changing body or environmental conditions. We report a biodegradable battery featuring a solid electrolyte of sodium chloride and polycaprolactone. This approach harnesses the body fluid that diffuses into the cell as an element of the electrolyte; however, the large excess of sodium chloride suspended in the polycaprolactone holds intracellular ionic conditions constant. A constant discharge profile can then be achieved even in the presence of varying external aqueous conditions, enabling compact, stable-performing cells. This design also features easy integration and automatic activation, providing a simplified strategy to fabricate batteries with long shelf life and desirable functional life span. In addition, the polymeric skeleton of the solid electrolyte system acts as an insulating layer between electrodes, preventing the metallic structure from short-circuit during discharge.

Keywords Biodegradable batteries · PCL · NaCl · Transient electronics · Stable performance · Automatic activation

1 Introduction

MEMS devices have been extensively used for sensing and modulation of a medical or environmental event to provide a means to improve patient health (Allen 2014) or sustain environmental protection. Many biocompatible MEMS devices, either passive or active, have achieved commercial success (Klosterhoff et al. 2017). Some typical examples include stents for treating narrowed arteries (Chow et al. 2010), actuators for pacing monitoring cardiovascular events (Chow et al. 2010; Dimarco 2003; Magalski et al. 2002), sensors for monitoring pollutants present in the atmosphere and in water

(Jackson et al. 2008; Baruah and Dutta 2009; Patel 2002; Suzuki 2000), and electrodes for neuromodulation (Chew et al. 2013; Kipke et al. 2003; Schmidt et al. 1996; Viventi et al. 2011; Rousche et al. 2001). In some cases, however, the medical or environmental need is transient; and as a result, permanent devices can persist long after they are needed. Such persistence can result in undesired problems; for example, in biomedical applications chronic implants can be susceptible to persistent inflammation and may require revision surgeries for device extraction after their functional lifetime. Recently emerging transient implantable medical devices (TIMDs) have garnered increasing interest due to their potential to eliminate the risks associated with permanent implants (Kim et al. 2010; Bettinger and Bao 2010; Yin et al. 2014) when treating or monitoring acute conditions. Specifically, TIMDs can breakdown into non-toxic components after a targeted lifespan, which excludes the need for revision surgery to remove the device and reduces the risk of chronic inflammatory response frequently observed with permanent implanted devices. This feature of TIMDs makes them more desirable in the monitoring and treatment of diseases and injuries that are transient in nature, such as bone fracture, traumatic brain injury, wound healing and drug delivery systems.

✉ Didi She
didishe@seas.upenn.edu

Mark Allen
mallen@seas.upenn.edu

¹ School of Engineering and Applied Science, University of Pennsylvania, Philadelphia, PA 19104, USA

² School of Biomedical Engineering, Georgia Institute of Technology, Georgia, GA 30332, USA

An example is the wireless radio frequency (RF) pressure sensor demonstrated by Luo et al. (2014). The sensor comprises zinc/iron bilayers as the sensor conductor material, and biodegradable polymers poly-L-lactide (PLLA) and polycaprolactone (PCL) as dielectric and structural materials. The functional lifetime of the sensors was approximately four days, and can be tailored by the choice of polymer encapsulation and ratio of the zinc/iron galvanic couple. Passive telemetry by analog inductive coupling is implemented in the operating frequency range of 10–100 MHz. Output power of the sensor is between 10–250 mW and the signal strength along the coil axis decreases as the third power of distance. Compared to chorionic devices, demonstrated TIMDs are still limited in functionality and application domain. There are many challenges that limit the development of biodegradable devices with more advanced functions and higher performance (Klosterhoff et al. 2017; Grayson et al. 2004; Bashir 2004). One prominent challenge is accommodating onboard powering to overcome the constraint of passive designs or wireless powering, and to support the design of self-powered TIMDs, which can potentially demonstrate higher performance over longer time intervals and exhibit greater functionality. Therefore, similarly biodegradable energy source is an essential component in developing biodegradable implants to facilitate handling transient injuries and diseases.

The work in energy sources featuring biodegradability and biocompatibility remains relatively unexplored. Researchers are still coming to grips with different types of transient batteries that offer output powers useful for the target class of devices (Yin et al. 2014; Heller 2006; Tsang et al. 2015; Jimbo and Miki 2008; Kim et al. 2013a, b; Park et al. 2009; Kim et al. 2014). Other practical challenges associated with the battery design include output stableness, device compactness and life time (including shelf life and operation life span) of the battery. Yin et al. (2014) demonstrated a series of biodegradable batteries featuring magnesium (Mg) as the anode, iron (Fe), molybdenum (Mo), or tungsten (W) as the cathode, and phosphate-buffered saline (PBS) as the electrolyte. This approach packaged all the battery components including the electrolyte within a cell and provided a constant electrochemical environment for stable operation of the battery. However, this structure incorporated liquid electrolyte at the expense of amenability to assembly and battery compactness. Electrolyte needs to be manually injected into the battery prior to implantation to eliminate corrosion of the electrodes for longer shelf life. In addition, this structure did not feature an insulating layer between anode and cathode, which might lead to short circuit of the electrodes within the liquid electrolyte. Jimbo and Miki (2008) reported an ingestible battery that is activated upon exposure to the gastric fluid, which eliminated the need to design for a bulky electrolyte and automatically simplified battery component integration and prolonged shelf life. While this approach achieved compactness by harnessing the surrounding body fluid, the electrochemical

cell design did not allow for encapsulation of the electrolyte to obtain stable battery performance in the presence of varying external aqueous conditions. The discharge profile of the battery was very unstable and the output current was susceptible to transient spikes.

This study presents the design, fabrication and testing of a biodegradable battery that satisfies the powering requirements for the target class of electronics and features easy integration, automatic activation, prolonged shelf life and improved stability. In our attempt to address the challenge of accommodating the bulk volume of the battery electrolyte, we integrated the anode/cathode pair with a solid electrolyte system that supports compact packaging. Specifically, this design comprises a Mg/Fe galvanic pair as the electrodes, and an immobilized electrolyte system which simultaneously utilizes body fluid as an element of the electrolyte. This approach harnessed the physiological solution by allowing a minimum amount of body fluid to penetrate and activate the battery, while maintaining a constant electrolytic environment within the cell for the stable powering of transient TIMDs.

2 Materials and methods

2.1 Battery design and working principle

The envisioned structure of the biodegradable battery is summarized in Fig. 1. The battery consists of two key functional components: (1) a Mg/Fe galvanic couple and (2) a NaCl/PCL electrochemical cell. Mg is incorporated as a sacrificial anode that galvanically protects an Fe cathode and powers the external device. NaCl particles are dispersed in PCL to form a solid system to serve as immobilized electrolyte, which defines the size of the battery. The top side of the NaCl/PCL cell is encapsulated by a laminated layer of PCL that dually serves as the packaging for the battery and a semipermeable membrane for infiltration of the electrolyte. A thick PLA film on the bottom side of the electrochemical cell, together with a PLA spacer, is used to emboss the electrode pair and confine the NaCl/PCL composite within the cell.

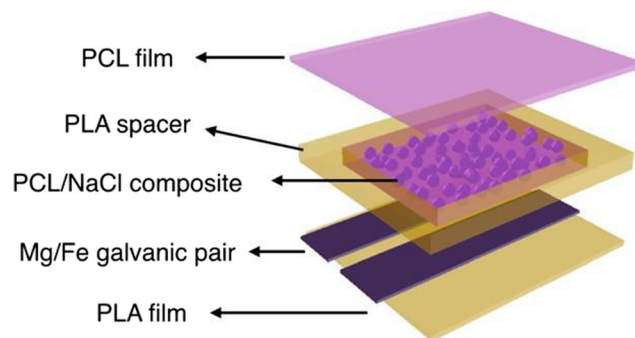
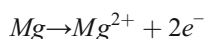
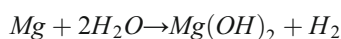


Fig. 1 Schematic diagram of immobilized electrolyte biodegradable battery

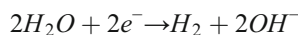
The constituent materials of the battery are all biocompatible, and spontaneously break down into non-toxic components after the functional life span of the battery (Witte et al. 2008; Langer 1998; Sodergard and Stolt 2002; Garlotta 2001; Zhu et al. 2009; Sun et al. 2006). Polycaprolactone is selected as the primary component of the solid electrolyte system due to its attractive chemical, mechanical, and physiological properties. Polycaprolactone has a very low glass-transition temperature (T_g) of about $-60\text{ }^\circ\text{C}$ and a melting temperature around $60\text{ }^\circ\text{C}$. Therefore, polycaprolactone is in the rubbery state at body temperature where it is soft and flexible and exhibits high permeability to low molecular weight species. In addition, polycaprolactone could be easily integrated with microfabrication techniques due to its low melting point and good solubility in a wide range of organic solvents including tetrahydrofuran, chloroform, acetone and ethyl acetate. Further, both polycaprolactone and polylactic acid have been demonstrated in long-term drug delivery systems and structural implants with confirmed biocompatibility *in vivo*. In turn, polylactic acid is selected as material for the supporting spacer structure because it has good tensile strength and is remarkably compatible with polycaprolactone. Sodium chloride is the ideal material for the electrolyte system since Na⁺ and Cl⁻ are the main ionic constituents of the body fluid. Mg/Fe galvanic couple is chosen as the anode/cathode pair because it has been previously investigated and proven to be a great candidate for the construction of biodegradable batteries. The anodic reaction of the electrochemical cell is given by:



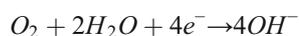
and the oxidation of Mg releases electrons into the external part of the circuit. The following side reaction also takes place on the anode and forms hydrogen gas and magnesium hydroxide ($\text{Mg}(\text{OH})_2$) simultaneously:



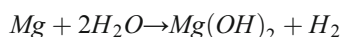
The cathodic reaction is dominated by hydrogen evolution:



while oxygen reduction reaction is limited by the amount of oxygen diffused onto the surface of the cathode. The following oxygen reduction is therefore considered as a side reaction in this article:



Consequently, the overall governing reaction of the battery is given by:



The activation of the battery requires the presence of water-based electrolyte to both act as a reactant on the cathode and

serve as an ionic pathway for the completion of the battery circuit. We have shown in our previous work (Tsang et al. 2015) that PCL film enables almost instantaneous penetration of physiological solution to activate the battery, and supports hydrogen diffusion. In the present design, the separate use of PCL in the encapsulating film and immobilized electrolyte permits greater flexibility in designing for electrochemical performance and compact packaging, as shown in Fig. 2. Much like a dry cell, liquid from the surrounding body permeates the immobilized electrolyte and activates the battery. The encapsulating PCL film would hinder the efflux of NaCl from the battery to confine the electrolyte within the electrochemical cell during battery discharge. Hydrogen gas formed during the battery discharge is released by diffusion across the thin PCL film. For longer functional time span of the battery, the PCL layer should selectively support water and hydrogen transport, but retard NaCl transport.

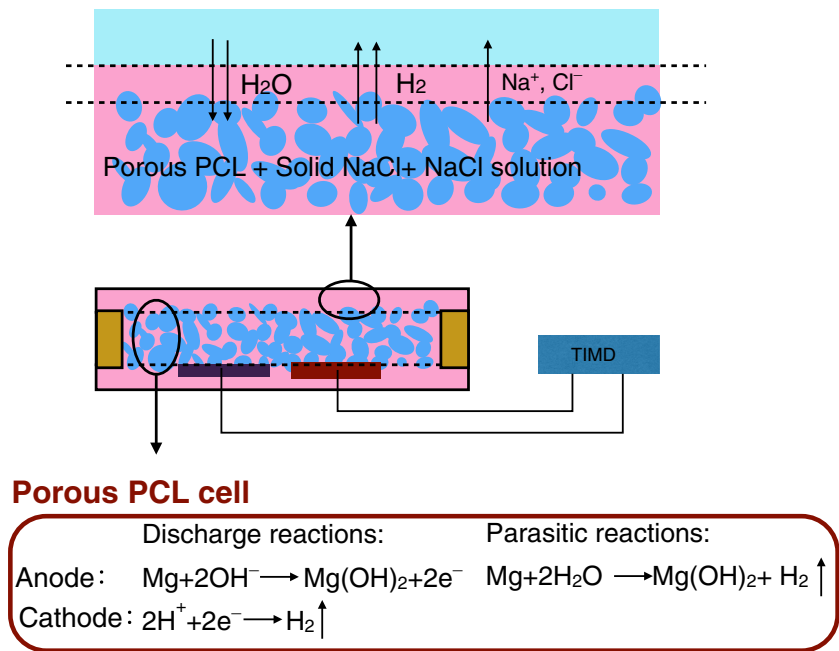
The schematic diagram of the circuit model representing the DC equivalence of the battery is shown in Fig. 3. The voltage V denotes the potential difference of the two half cells of the battery which varies with the parasitic reactions on the electrodes. A leakage path enabled by the parasitic corrosion reaction on the anode is denoted by the serial connection of R_1 and R_3 . When a closed loop circuit is formed at the terminals, the discharge current drawn from the battery flows through R_1 and R_2 and powers the external device. In the discharge loop, R_1 denotes the ohmic resistance of the battery which describes the polarization resistance and electrolyte resistance in the cell. R_2 denotes the electrolyte resistance and connection resistance of the battery. The cumulative effect of side reactions need to be considered when understanding the parameters in the circuit model and evaluating the performance of battery.

2.2 Fabrication and assembly

The fabrication process of the immobilized electrolyte biodegradable battery is schematically shown in Fig. 4. The PCL/NaCl composite was prepared by solvent-casting. Commercial 80 kDa PCL pellets were solubilized in acetone at a concentration of 100 mg/mL. 150 g sodium chloride (NaCl) with a particle size of 300–400 μm was dispersed in 100 mL PCL solution and casted. The composites were dried under ambient conditions for 24 hours and vacuum-dried to remove residual solvent for an additional 12 hours.

To define the solid electrolyte shape, a polylactic acid (PLA) spacer was fabricated using 3-D printing technology (Makerbot Replicator 2X). PLA was selected due to its high processing temperature (approximately $180\text{ }^\circ\text{C}$), which is inert to the following high temperature process of PCL. The solid electrolyte was molded into the PLA spacer with a lamination press at $65\text{ }^\circ\text{C}$, which is above the PCL melting point (approximately $61\text{ }^\circ\text{C}$). The PCL/NaCl composite (93.75 wt% NaCl) then softened and adopted the shape defined by the spacer.

Fig. 2 The principle of operation of the biodegradable battery. Liquid absorbed into the cell activates the battery by converting solid NaCl into a super saturated NaCl solution. Na⁺ and Cl⁻, as well as hydrogen gas, leach out from the PCL film. The governing chemistry in the electrolytic cell is the cathodic protection of Fe through the oxidation of Mg anode and, parasitic corrosion of the Mg



Next, the Mg and Fe electrode pair was embossed onto one surface of the battery and encapsulated with an PLA film. Finally, a thin PCL film is laminated onto the opposite surface of the PCL/NaCl composite at 65 °C to seal the battery.

2.3 Characterization and testing

The permeability of NaCl in PCL films was characterized to support design of the battery packaging. Samples used to evaluate the barrier properties of the PCL structure were fabricated with same geometries as those used in the battery, except that no electrodes were incorporated. Samples were immersed in a large volume of deionized (DI) water (250 mL) to (1) establish zero concentration conditions of NaCl external to the battery and (2) minimize concentration changes in the external environment. At periodic time points, the samples were removed from the liquid, air-dried at slightly increased temperature (e.g. 35°C) for 12 hr, and weighed to determine the rate of NaCl transport across the polymers. As discussed, the PCL layer should selectively support water and hydrogen

transport, but retard NaCl transport. As high mass transfer resistance of NaCl is required to retain the electrolyte within the battery, PCL films with varying thicknesses were compared to determine the optimum parameters that satisfy these mass transfer and battery discharge design constraints.

To further understand the role of water and its influence on the discharging behavior, batteries were tested under constant load discharge in a DI water environment. The batteries were dipped into water to evaluate the activation behavior. Additionally, after the battery stabilized after a certain period of time, it was removed from water to evaluate the deterioration in performance originated from loss of water. After the potential fell below the cutoff point, the battery was immersed in water for the second time to observe the subsequent performance of the battery.

The electrochemical performance of the battery was tested under galvanostatic conditions in a two-electrode-cell configuration at various discharge rates up to 0.1 mA/cm² using a potentiostat (WaveDriver 10, Pine Instruments). The batteries were discharged in 100 mL of SBF at 37 °C to emulate the

Fig. 3 The schematic diagram of the circuit model

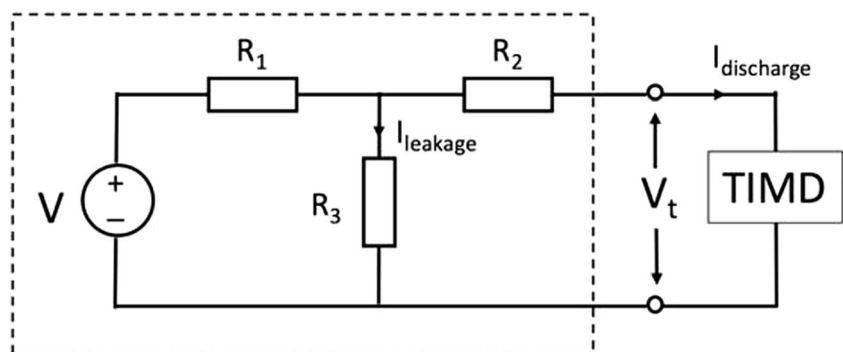
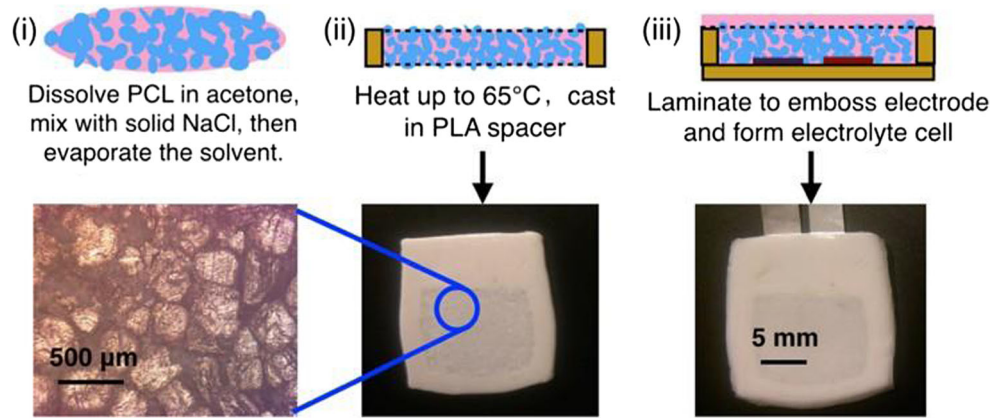


Fig. 4 Fabrication process of the battery



physiological environment. The internal resistance (R_i) and the open circuit voltage (V_{oc}) of the battery can be investigated using the following equation:

$$V_t = V_{oc} - R_i \cdot I \tag{1}$$

where V_{oc} , I , R_i and V_t refer to the open circuit potential (V), discharge current (A), internal resistance (Ω), and output voltage (V) at the terminals of the cell, respectively.

In addition, the batteries were tested in a series of liquids (i.e., either DI water, 0.1 M NaCl, and SBF) to investigate how the external ionic environment affects the ionic transport across the PCL encapsulation and stability of the immobilized electrolyte within the battery. The battery was first activated in DI water and discharged at a constant current of $25 \mu\text{A}/\text{cm}^2$. After 1 hour of stable discharge, the battery was removed from the DI water and immediately immersed into the NaCl solution. After another hour of stable discharge, the battery was immersed into SBF solution. Finally, the solution was again changed to DI water after another hour of stable discharge.

The solution volumes were 200 mL and tests were performed under room temperature.

3 Results and discussion

3.1 Characterization of battery components

Figure 4 shows optical images of the PCL/NaCl composite and the configuration of the battery. The simple structure of the battery facilitates miniaturization. It is designed to have a volume approximately defined by the solid electrolyte system. The geometry of the presented batteries is depicted in Fig. 2. The battery has a solid electrolyte volume of $12 \text{ mm} \times 10 \text{ mm} \times 2 \text{ mm}$, which contains 0.48g NaCl/PCL composite (93.75 wt% NaCl), and the total size of the fabricated battery is $16 \text{ mm} \times 16 \text{ mm} \times 2 \text{ mm}$. Mg foil with 0.45 cm^2 active area and thickness of $45 \mu\text{m}$ was put into the battery, and the anode cathode spacing was 1 mm.

Fig. 5 NaCl leach rate of the NaCl/PCL composite structure with top PCL membrane thickness of $0 \mu\text{m}$, $20 \mu\text{m}$, $50 \mu\text{m}$, $80 \mu\text{m}$, respectively

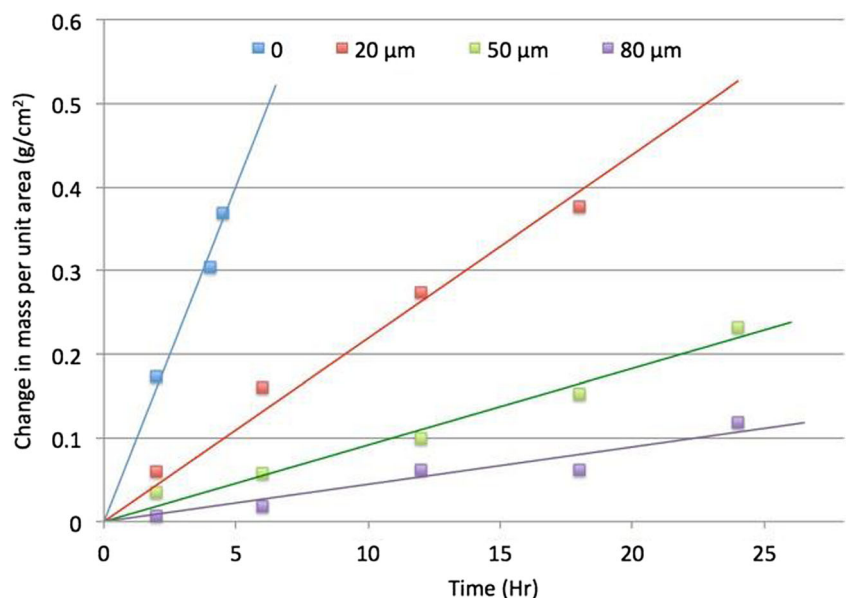
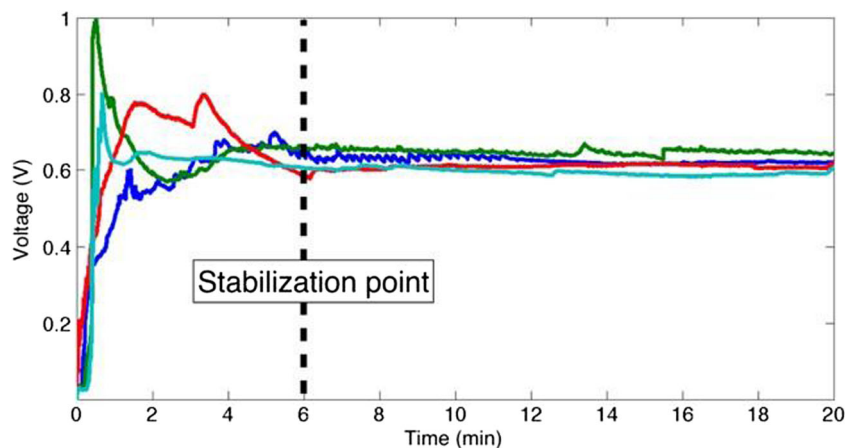


Fig. 6 Discharge behavior upon activation of four batteries with the same configuration and discharge parameters



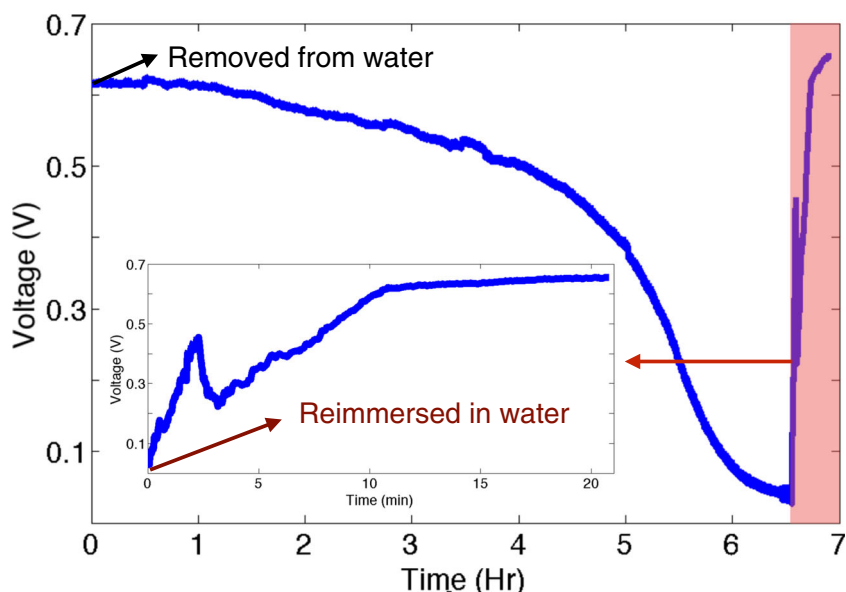
Towards finding the optimum coating area and thickness of the PCL film for hindering NaCl efflux from the NaCl/PCL composite without appreciably increasing the mass transfer resistances of hydrogen and water, NaCl permeability tests were conducted to evaluate its diffusion properties in PCL. As shown in Fig. 5, the leaching of NaCl from the battery is hindered by the polymeric binder in the NaCl/PCL composite, as well as the PCL membrane encapsulating the composite. The leach rate of NaCl across 20 μm and 50 μm membranes were approximately 22 mg/cm²/h and 9 mg/cm²/h, respectively. These findings showed that the lifetime of the battery is limited by depletion of the active material (Mg), as well as loss of the solid electrolyte. For a battery to last more than 24 hr, a membrane between 30 μm and 50 μm thick has been experimentally determined to be the optimum coating thickness for maximizing the stability and performance of the batteries. In addition, the battery depicted in Fig. 3 contains 0.45 g NaCl, which could support stable discharge for about 40

hours, and 4 mg Mg, indicating that the battery lifetime in this configuration is limited by depletion of the anode.

Figure 6 demonstrates the discharge behavior upon activation in DI water of four batteries with the same thickness of PCL membranes (30 μm). The output voltage of the battery statistically stabilized in 6 minutes, which demonstrated that the PCL structure allows sufficient water transport for activation of the battery. Increasing the PCL thickness to 50 μm was experimentally proven to not appreciably prolong the activation time of the battery.

After the battery was stabilized in DI water and discharged for 24 hours, it was removed from the water and continued with discharging. Figure 7 shows that the liquid retained in the cell supported continued discharge for up to 6 hours in air. When the discharge potential fell below a cutoff potential of 0.1 V, immersion of the battery in water enabled the battery to resume to the steady state discharge potential after 10 minutes, verifying that the voltage decline or termination of the battery

Fig. 7 Discharge behavior of a battery removed from DI water after being discharged for 24 h. The battery terminates in 6 h due to liquid loss, and resumes its performance shortly after reimmersion in water for a second time



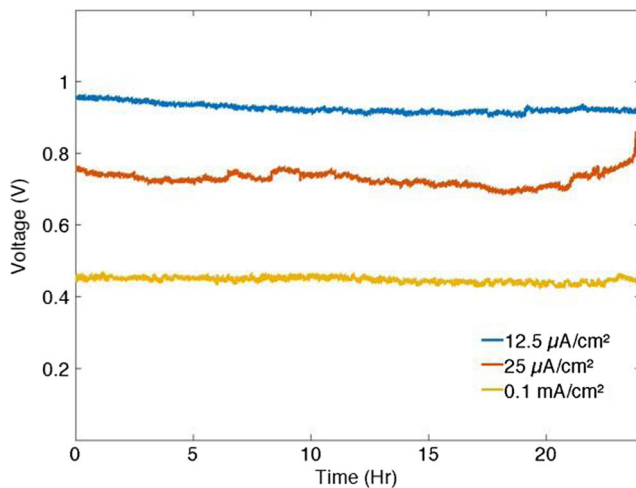


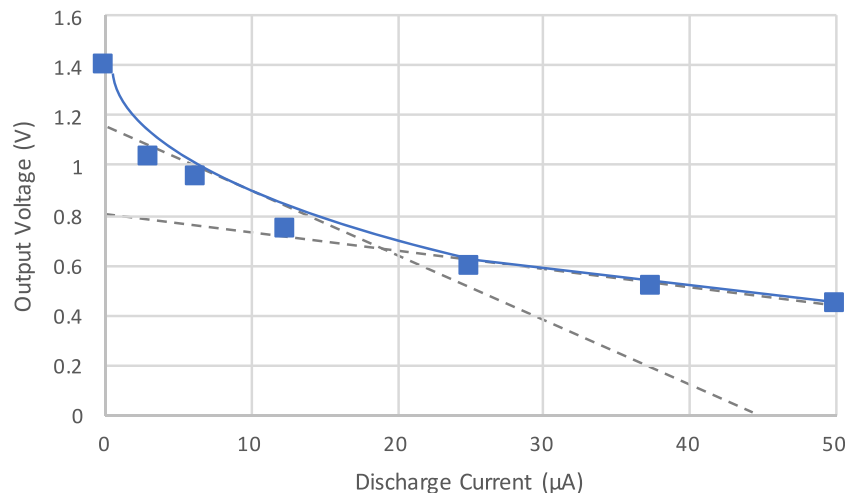
Fig. 8 Discharging behavior under constant current. The operating voltages are approximately 0.95 V, 0.75 V and 0.45 V for discharge rates of $12.5 \mu\text{A}/\text{cm}^2$, $25 \mu\text{A}/\text{cm}^2$ and $0.1 \text{ mA}/\text{cm}^2$, respectively

was caused by the consumption of water inside the battery. The deterioration in battery performance was due to the loss of water, as water is consumed in the governing reactions of the battery, as well as undergoes evaporation. These findings suggested that the PCL structure offers functional advantages for retaining the electrolyte even in air. Further, the PCL film was mechanically robust to accommodate for releasing of hydrogen during the discharge of the battery for prolonged periods. It was also speculated that capillary force contributes to the fast absorbance of water, especially in the second immersion, and internal pressure might have contributed to the release of hydrogen from the PCL membrane.

3.2 Electrochemical testing of biodegradable batteries

To emulate the *in vivo* environment where the battery would be surrounded by physiological fluid, electrochemical testing

Fig. 9 Battery terminal voltage at different discharge currents. V_t changes nonlinearly with I at smaller currents



was conducted in SBF, as its composition approximates the inorganic content of human blood plasma. The discharge behavior with a PCL membrane thickness of $50 \mu\text{m}$ is shown in Fig. 8. The operating voltages are approximately 0.95 V, 0.75 V and 0.45 V for discharge rates of $12.5 \mu\text{A}/\text{cm}^2$, $25 \mu\text{A}/\text{cm}^2$ and $0.1 \text{ mA}/\text{cm}^2$, respectively. In each case, the terminal voltage is stable for at least 24 hours during the constant-current discharge. The current is linearly related to the voltage in relation to Ohm's law, which indicates that in applications involving a purely resistive load, the output current would still be fairly constant.

Figure 9 illustrates how the battery behaves at different discharge currents. As discussed, the open circuit potential and internal resistance are related to terminal voltage and discharge current as described by equation (1). In this case, V_t changes nonlinearly with I , which leads to a varying V_{oc} and R_i at different discharge currents. At each current point, transient V_{oc} and R_i can be determined using an assisting tangent line, of which the absolute value of the gradient is equal to R_i , and the intercept on the y-axis is equal to V_{oc} . Note that at increased discharge currents, there is a decline in both V_{oc} and R_i , as indicated by the dotted line. It is speculated that the higher V_{oc} and R_i observed at lower discharge current is attributed to the corrosion mechanism of magnesium. It has been previously demonstrated in other literatures (Tsang et al. 2015; Witte et al. 2008; Xue et al. 2012) that magnesium features a passivation layer of $\text{Mg}(\text{OH})_2$ at the surface, and the discharge chemistry relies on the continuous formation and breakdown of the passivation layer. The formation of poorly soluble $\text{Mg}(\text{OH})_2$ film hinders the corrosion of magnesium, which may lead to both high leakage and discharge path resistances at low discharge rate. When a current is drawn from the battery, the $\text{Mg}(\text{OH})_2$ layer is mechanically disrupted to expose the underlying magnesium. As the current increases, the rate of film breakdown overcomes the rate of $\text{Mg}(\text{OH})_2$ reformation, which subsequently leads to a decrease in internal resistance.

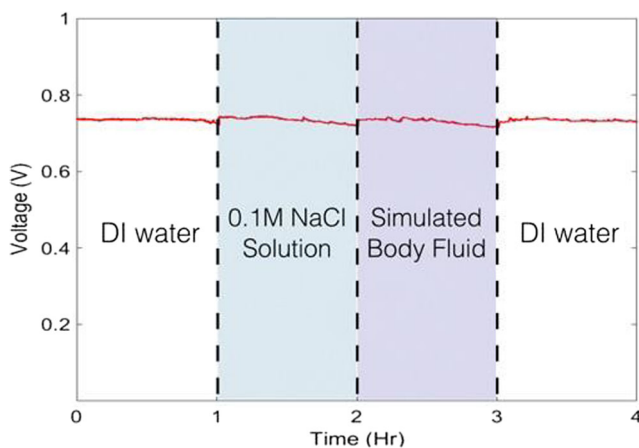


Fig. 10 Discharging behavior under a constant current of $25 \mu\text{A}/\text{cm}^2$. The liquid volume outside of the battery was changed every one hour

Physiological fluid, such as human blood plasma, comprises mainly of water (up to 95% v/v) and inorganic salts (e.g., NaCl). To demonstrate that the immobilized electrolyte approach renders the biodegradable battery immune to the external liquid environment, Fig. 10 shows the discharge of a battery sequentially in DI water, 0.1 M NaCl, and SBF. Further, the liquid solutions selected increasingly approximate the composition of human blood plasma. Hence, the stable discharge profile achieved from this experiment suggested that the performance of the presented battery is not susceptible to the surrounding physiological environment.

4 Conclusions

This study detailed an approach to achieving a biodegradable battery with immobilized electrolyte for transient implantable medical devices. Specifically, the battery features a Mg/Fe galvanic pair as the electrodes, and encapsulates a solid system comprising NaCl dispersed in a polymeric (PCL) volume. Since the ionic concentration within the encapsulation is high, the cell performance is reasonably independent of external environment as long as the internal moisture content and NaCl concentration remain above a threshold. This approach harnesses bodily fluid as an element of the electrolyte, thereby features auto activation of the battery and reduces processing complexity of sealing liquid within a cell. Besides, since the cell is ‘dry’ prior to implantation, this design eliminates concerns with shelf life and unwanted corrosion prior to desired use of the battery. Moreover, the battery encapsulation provides a barrier for retaining the electrolyte and potentials of preventing influx of large organic molecules, and the cell structure naturally prevents the short circuit of the electrodes. In addition, since the electrolyte is highly concentrated salt, the activity of the electrolyte space can be maintained at the saturation concentration of NaCl, thus providing the desired constant environment to support stable battery performance.

Acknowledgements The work was supported by the National Institute of Health (R21-AR066322) and the National Science Foundation (CMMI-1362652). Microfabrication was carried out at the Singh Center for Nanotechnology, which is supported by the NSF National Nanotechnology Coordinated Infrastructure Program under grant 15-42153.

Publisher’s note Springer Nature remains neutral with regard to jurisdictional claims in published maps and institutional affiliations.

References

- M. G. Allen, Microfabricated implantable wireless microsystems: Permanent and biodegradable implementations, Proc. IEEE Int. Conf. Micro Electro Mech. Syst., pp. 1–4 (2014)
- S. Baruah, J. Dutta, Nanotechnology applications in pollution sensing and degradation in agriculture. *Environ. Chem. Lett.* **7**(3), 191–204 (2009)
- R. Bashir, BioMEMS: State-of-the-art in detection, opportunities and prospects. *Adv. Drug Deliv. Rev.* **56**(11), 1565–1586 (2004)
- C.J. Bettinger, Z. Bao, Biomaterials-based organic electronic devices. *Polym. Int.* **59**(5), 563–567 (2010)
- D.J. Chew, L. Zhu, E. Delivopoulos, I.R. Mineev, K.M. Musick, C.A. Mosse, M. Craggs, N. Donaldson, S.P. Lacour, S.B. McMahon, J.W. Fawcett, A microchannel Neuroprosthesis for bladder control after spinal cord injury in rat. *Sci. Transl. Med.* **5**(210), 210 (2013)
- E.Y. Chow, A.L. Chlebowski, S. Chakraborty, W.J. Chappell, P.P. Irazoqui, Fully wireless implantable cardiovascular pressure monitor integrated with a medical stent. *IEEE Trans. Biomed. Eng.* **57**(6), 1487–1496 (2010)
- J.P. Dimarco, Implantable Cardioverter–Defibrillators. *N. Engl. J. Med.* **349**(19), 1836–1847 (2003)
- D. Garlotta, A literature review of poly(lactic acid). *J. Polym. Environ.* **9**(2), 63–84 (2001)
- A.C.R. Grayson, R.S. Shawgo, A.M. Johnson, N.T. Flynn, Y. Li, M.J. Cima, R. Langer, A BioMEMS review: MEMS technology for physiologically integrated devices. *Proc. IEEE* **92**(1), 6–21 (2004)
- A. Heller, Potentially implantable miniature batteries. *Anal. Bioanal. Chem.* **385**(3), 469–473 (2006)
- T. Jackson, K. Mansfield, M. Saafi, T. Colman, P. Romine, Measuring soil temperature and moisture using wireless MEMS sensors. *Measurement* **41**(4), 381–390 (2008)
- H. Jimbo, N. Miki, Gastric-fluid-utilizing micro battery for micro medical devices. *Sensors Actuators B Chem.* **134**(1), 219–224 (2008)
- D. H. Kim, J. Viventi, J. J. Amsden, J. Xiao, L. Vigeland, Y.-S. Kim, J. A. Blanco, B. Panilaitis, E. S. Frechette, D. Contreras, D. L. Kaplan, F. G. Omenetto, Y. Huang, K.-C. Hwang, M. R. Zakin, B. Litt, and J. A. Rogers, “Dissolvable films of silk fibroin for ultrathin conformal bio-integrated electronics,” *Nat. Mater.* **9**(6), 511–517 (2010)
- Y.J. Kim, S.-E. Chun, J. Whitacre, C.J. Bettinger, Self-deployable current sources fabricated from edible materials. *J. Mater. Chem. B* **1**(31), 3781 (2013a)
- Y. J. Kim, W. Wu, S.-E. Chun, J. F. Whitacre, and C. J. Bettinger, Biologically derived melanin electrodes in aqueous sodium-ion energy storage devices., *Proc. Natl. Acad. Sci. U. S. A.*, vol. 110, no. 52, pp. 209 (2013b), 20912
- Y.J. Kim, W. Wu, S.E. Chun, J.F. Whitacre, C.J. Bettinger, Catechol-mediated reversible binding of multivalent cations in eumelanin half-cells. *Adv. Mater.* **26**(38), 6572–6579 (2014)
- D.R. Kipke, R.J. Vetter, J.C. Williams, J.F. Hetke, Silicon-substrate intracortical microelectrode arrays for long-term recording of neuronal spike activity in cerebral cortex. *IEEE Trans. Neural Syst. Rehabil. Eng.* **11**(2), 151–155 (2003)

- B. S. Klosterhoff, M. Tsang, D. She, K. G. Ong, M. G. Allen, N. J. Willett, and R. E. Guldberg, Implantable sensors for regenerative medicine, *J. Biomech. Eng.*, vol. 139, no. 2, p. 21009 (2017), 021009
- R. Langer, Drug delivery and targeting. *Nature* **392**(6679), 5–10 (1998)
- M. Luo, A.W. Martinez, C. Song, F. Herrault, M.G. Allen, A microfabricated wireless RF pressure sensor made completely of biodegradable materials. *J. Microelectromech. Syst.* **23**(1), 4–13 (2014)
- A. Magalski, P. Adamson, F. Gadler, M. Böehm, D. Steinhaus, D. Reynolds, K. Vlach, C. Linde, B. Cremers, B. Sparks, T. Bennett, Continuous ambulatory right heart pressure measurements with an implantable hemodynamic monitor: A multicenter, 12-month follow-up study of patients with chronic heart failure. *J. Card. Fail.* **8**(2), 63–70 (2002)
- J. Park, J. Chang, S. Ahn, Y.K. Pak, S. Han, J.J. Pak, Array type dissolved oxygen sensor and measurement system for simultaneous measurement of cellular respiration level, International Solid-State Sensors, Actuators and Microsystems Conference (Transducers 2009), Denver, (2009)
- P.D. Patel, (bio)sensors for measurement of analytes implicated in food safety: A review. *Trends Anal. Chem.* **21**(2), 96–115 (2002)
- P.J. Rousche, D.S. Pellinen, D.P. Pivin, J.C. Williams, R.J. Vetter, D.R. Kipke, Flexible polyimide-based intracortical electrode arrays with bioactive capability. *IEEE Trans. Biomed. Eng.* **48**(3), 361–370 (2001)
- E.M. Schmidt, M.J. Bak, F.T. Hambrecht, C.V. Kufta, D.K. O'Rourke, P. Vallabhanath, Feasibility of a visual prosthesis for the blind based on intracortical microstimulation of the visual cortex. *Brain* **119**(5), 507–522 (1996)
- A. Sodergard, M. Stolt, Properties of lactic acid based polymers and their correlation with composition. *Prog. Polym. Sci.* **27**(6), 1123–1163 (2002)
- H. Sun, L. Mei, C. Song, X. Cui, P. Wang, The in vivo degradation, absorption and excretion of PCL-based implant. *Biomaterials* **27**(9), 1735–1740 (2006)
- H. Suzuki, Microfabrication of chemical sensors and biosensors for environmental monitoring, **12**, 1–2, pp. 55–61 (2000)
- M. Tsang, A. Armutlulu, A. W. Martinez, S. A. B. Allen, and M. G. Allen, Biodegradable magnesium/iron batteries with polycaprolactone encapsulation: A microfabricated power source for transient implantable devices, *Microsystems Nanoeng.*, vol. 1, no. August, p. 15024 (2015)
- J. Viventi, D.-H. Kim, L. Vigeland, E.S. Frechette, J. a Blanco, Y.-S. Kim, A.E. Avrin, V.R. Tiruvadi, S.-W. Hwang, A.C. Vanleer, D.F. Wulsin, K. Davis, C.E. Gelber, L. Palmer, J. Van der Spiegel, J. Wu, J. Xiao, Y. Huang, D. Contreras, J. a Rogers, B. Litt, Flexible, foldable, actively multiplexed, high-density electrode array for mapping brain activity in vivo. *Nat. Neurosci.* **14**(12), 1599–1605 (2011)
- F. Witte, N. Hort, C. Vogt, S. Cohen, K. U. Kainer, R. Willumeit, and F. Feyerabend, Degradable biomaterials based on magnesium corrosion, **12**, 5–6 (2008)
- D. Xue, Y. Yun, Z. Tan, Z. Dong, M.J. Schulz, In vivo and in vitro degradation behavior of magnesium alloys as biomaterials. *J. Mater. Sci. Technol.* **28**(3), 261–267 (2012)
- L. Yin, X. Huang, H. Xu, Y. Zhang, J. Lam, J. Cheng, J.A. Rogers, Materials, designs, and operational characteristics for fully biodegradable primary batteries. *Adv. Mater.* **26**(23), 3879–3884 (2014)
- S. Zhu, N. Huang, L. Xu, Y. Zhang, H. Liu, H. Sun, Y. Leng, Biocompatibility of pure iron: In vitro assessment of degradation kinetics and cytotoxicity on endothelial cells. *Mater. Sci. Eng. C* **29**(5), 1589–1592 (2009)